

EFFECT OF SPACE CONFIGURATION OF BUILDING ON TSUNAMI FORCE ON IT

Norimi Mizutani¹, Satoru Aoki², Chathura Manawasekara¹ and Tomoaki Nakamura¹

Tsunami evacuation building is an important countermeasure in saving lives from tsunami inundation in coastal area. In the design of tsunami evacuation building, it is important to evaluate its stability against tsunami impact. However, openings like windows or pilotis may affect the tsunami force significantly and therefore it is important to discuss the effect of space configuration of the buildings on acting tsunami force. In this study, hydraulic model experiments and numerical simulation have been conducted to investigate on that aspect. Results show that spatial configuration of the building affects the total tsunami force acting on the structure. Numerical results also provided a good estimation of pressure distribution which agrees with experimental results.

Keywords: tsunami force; evacuation building; space configuration

INTRODUCTION

According to the damage observations from recent-past major tsunami events it is clearly evident that majority of the coastline protection structures that had been installed, including coastline buildings, were ineffective in standing against the giant wave. Especially, with narrow and limited evacuation time due to the near tsunami source has forced to find the evacuation shelters within the flat coastland. Meantime, the damage and failure of reinforced concrete structures under tsunami loading have increased the wreckage and also have degrade the possibility of effective evacuation. Therefore the resistance and stability of coastal structures such as evacuation are immensely valued.

Various types of failures to the buildings have been observed by number of researchers including damage observations to the coastal buildings by Nakano (2008) in the aftermath of 2004 Indian Ocean tsunami and categorization of the damage to reinforced concrete buildings during the 2011 Tohoku earthquake tsunami by Nishiyama et al. (2011), through the results observed in the field surveys. Studies have highlighted the importance of revising the existing coastal building design methods to meet an effective structural design to provide more resilience against the tsunami wave.

Therefore, existing design equations for the tsunami force estimation on coastal buildings require further investigations to incorporate different aspects of structural arrangement and configurations of the building. Asakura et al. (2000) and Arikawa et al. (2005) conducted experimental study on wave force acting on coastal structures by tsunami wave. Based on their experiments, Asakura et al. (2000) proposed an empirical formula to estimate the maximum tsunami wave pressure acting on the structures (Eq. 1). In the tsunami evacuation building design guideline published by Cabinet office of Japanese government (2005) the acting tsunami pressure is calculated considering the hydrostatic pressure distribution for a flow depth three times than of maximum tsunami inundation depth, based on Asakura et al. (2000). The primary intention of this method is to invisibly include the dynamic effects in to hydrostatic pressure calculations without more complications.

$$P_{\max}(z) = (3\eta_{\max} - z)\rho g \quad (1)$$

where, P_{\max} is the maximum tsunami wave pressure ($0 \leq z/\eta_{\max} \leq 3$); z is the height from the ground level; η_{\max} is the maximum inundation depth; ρ is the density of water; and g is the gravitational acceleration.

Further, Lukkunaprasit et al. (2009) conducted 1:100 scale physical model experiments to understand the effect of openings to the resulting tsunami force on vertical tsunami evacuation shelters. The study highlighted the reduction of tsunami force with the presence of openings in the building compare to that of a fully enclosed one. However further studies are needed to incorporate the effect of openings in to the design tsunami force estimation equations in order to proceed towards a more effective design guideline for coastal buildings like emergency evacuation shelters, which can be used under a tsunami threat. In the current study three-dimensional hydraulic experiments were conducted with the aim of assessing the effect of spatial configurations of the building in the estimation of tsunami force on it.

¹ Civil Engineering Department, Nagoya University, Furo-cho, Chikusa-ku, Nagoya, Aichi, 464-8603, Japan

² Power Generation Division, Hokkaido Electric Power Co., Inc., Chuo-ku, Sapporo, Hokkaido, 060-8677, Japan

Wave Condition	Wave type	Wave period (s)	Wave height (cm)	Tsunami flow type
Wave 1	Long period wave	20	3	Non-breaking
Wave 2			4	Non-breaking
Wave 3		15	3	Non-breaking
Wave 4			4	Non-breaking
Wave 5			5.5	Bore
Wave 6		10	3	Non-breaking
Wave 7			5.5	Bore
Wave 8			8	Bore
Wave 9	Half of sinusoidal wave		7	Breaking wave
Wave 10			12	Breaking wave
Wave 11			17	Breaking wave

EXPERIMENT STUDY

Physical experiments were carried out in the wave flume (30 m in length, 0.7 m in width and 0.9 m in height) of Department of Civil Engineering, Nagoya University. Experimental set-up was prepared according to the Froude similitude law with a scale of 1:50. Tsunami was generated with a piston type wave generator and the inclination of impermeable bed was kept as 1/10 as shown in the Fig. 1, while rest of the bed area was maintained to be horizontal. Ten wave gauges were installed at the positions indicated in the Fig. 1 to measure the tsunami wave height. The whole experiment procedure was recorded using a digital video camera placed in align with the centerline of the flume just off the shoreline and above the free water surface.

The maximum stroke of 1.5 m of the wave generator was employed in generating long period waves while half of sinusoidal waves were also yielded in producing different tsunami conditions of the on-land flow. Three main flow conditions were considered depending upon the wave profile and the inundation speed of the tsunami, as shown in the Table 1. The 'Non-breaking' type represents the situation where the tsunami overflows with slow speed, while the 'Bore' represents the tsunami overflows with a relatively higher speed, and the third type of 'Breaking wave' case was used to reproduce the condition where tsunami wave break in front of the structure.

Three types of configurations were considered for the building models, depending upon the special arrangement of the structural elements within the building. The general outer dimensions of the building model which constructed with 10 mm thick acrylic plates, was 400 mm × 320 mm × 270 mm. The model without any openings on either side was considered as building type 'A' (Fig. 1). The structure was modeled in the height of three story and the remaining two types of building frames were as similar outer dimensions as building 'A' but varied with the openings and the spatial arrangement inside the main frame. Building type 'B' (Fig. 3) was considered as a structure with only windows in either side of each story and building type 'C' consisted of array of pillars in the 1st story (ground level) and windows on either side of the building for the remaining two stories. These particular types were selected for the study depending upon the variety of general building types, which available in the

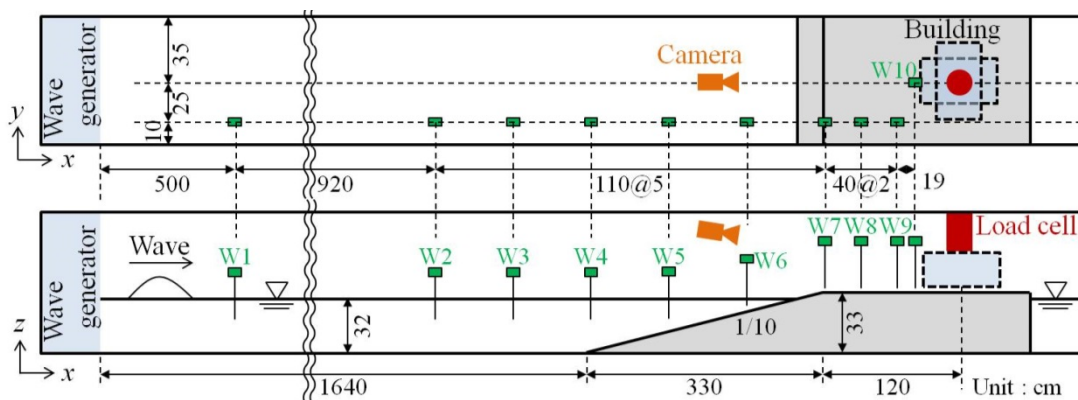


Figure 1. Three-dimensional view of building type 'A' with outer dimensions

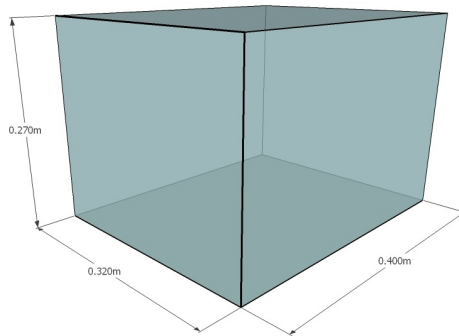


Figure 2. Three-dimensional view of building type 'A' with outer dimensions

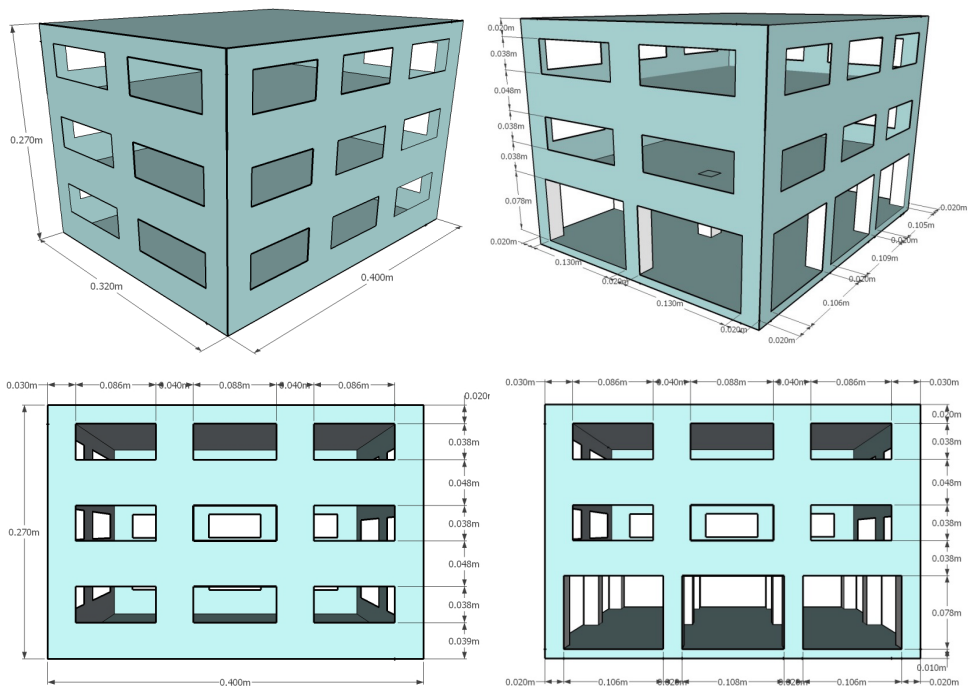


Figure 3. Three-dimensional view of building type 'B' (left) and building type 'C' (right) with outer dimensions

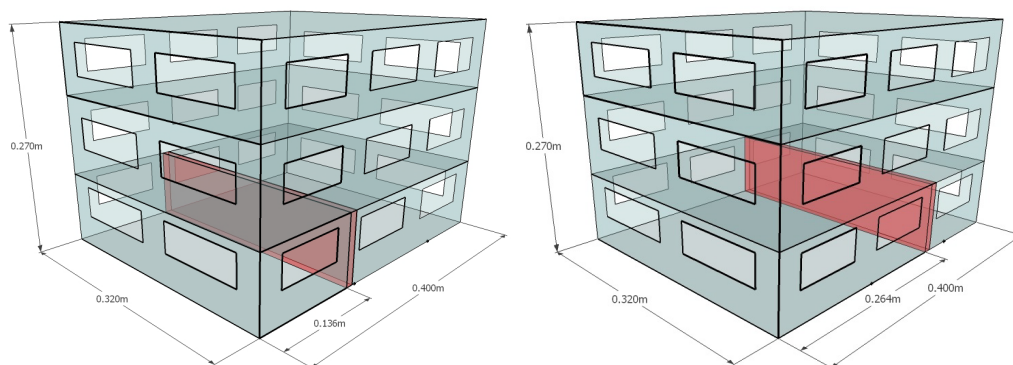


Figure 4. Arrangement of the separation wall at the ground floor

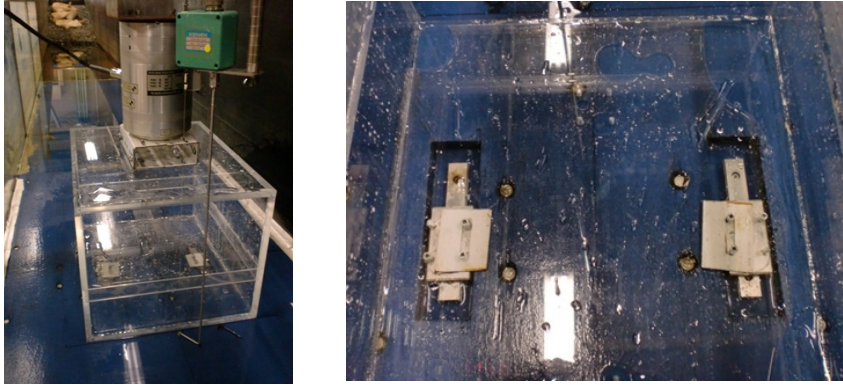


Figure 5. Arrangement of the force transducer on top of the model (left) and the view from the top at the glider arrangement at the bottom of the model

coastal zone, and considering suggestions and recommendations from previous studies.

Two arrangements for the each building model at the installed location were considered in the experiment as width side (shorter dimension) of the building facing tsunami (orientation 1) and the length side of the building facing tsunami (orientation 2) as in Fig. 1 (top). For the building 'B' and building 'C' additional two configurations were allocated taking the service requirements into account. Accordingly, a living compartment was created by adding a wall segment in the direction perpendicular to the tsunami flow, in the 1st floor. Two types of living compartment arrangements were introduced based on the location of the particular wall and positioning of the separation wall segment for the building 'B' is shown in the Fig. 4. Also, similar positions were selected for the wall in the building 'C'. Additionally, a service location for an elevator shaft also allocated in the building models 'B' and 'C'. The arrangement of service configurations and the notations used in the experiment for each case are shown in Fig. 6.

Pressure on each type of building models exerted by tsunami impingement was measured using five pressure sensors placed in line in the vertical direction at distance of 0.6 cm each and the location of the pressure sensor arrangement for each case is shown by the yellow dot in Fig. 6. The signals from the pressure sensors were treated with a low pass filter to reduce the noise prior to the analysis. At the same time, the measurements for a particular condition were taken three times in order to avoid any sort of variation due to an associated error.

Force transducer for the measurement of the total force acting on the building due to tsunami impact, was installed on top of the structure by supporting from the top, and measurements were taken only for the exerted force on the tsunami flow direction (x -direction). Fig. 5 (left) shows the placement of the force gauge on top of the building model, in the experiment set-up.

Additionally, pair of gliders was installed underneath the structure [Fig. 5 (right)] allowing the building to move in x -direction following the tsunami impingement, while restraining movement in any other directions. The resultant force required to stop the x -directional movement was detected by the force transducer and taken as the acting external force on the structure. The original output from the force gauge was passed through a low-pass filter in order to reduce the amount of noise associated with

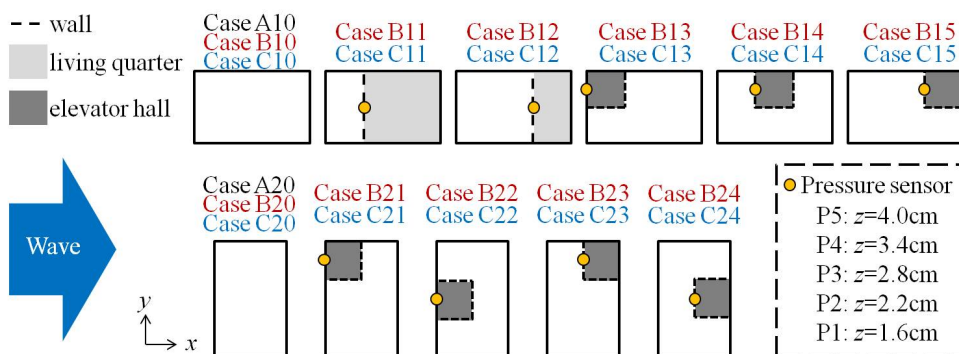


Figure 6. Cases considered depend on the internal arrangement

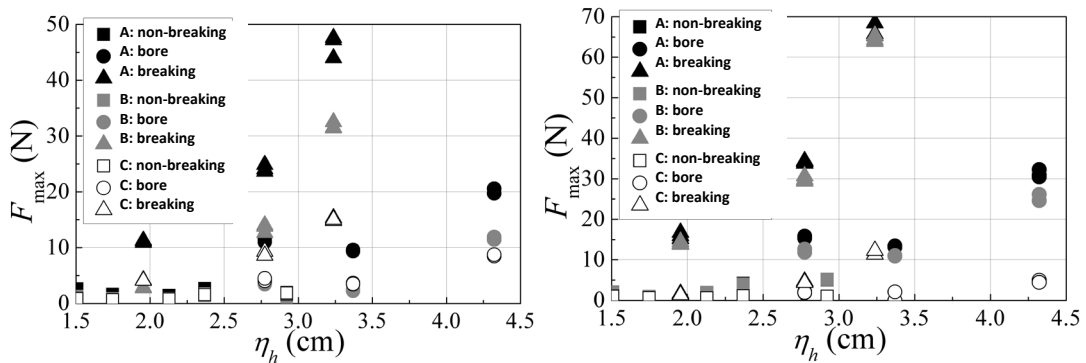


Figure 7. Maximum wave force against maximum wave height; for width side facing tsunami (left) and length side facing tsunami (right)

the measurements.

EXPERIMENT RESULTS

Effect of the Openings on Tsunami Force

Fig. 7 show the maximum tsunami force (F_{max}) against the maximum wave height observed at the location of the structure (η_h), for the cases where width side of the structure facing tsunami and the length side of the structure facing tsunami, respectively. Here, the cases with inner wall or elevator are not considered. By looking at the figures it can be clearly noticed that F_{max} is higher for the breaking wave type when compare to the non-breaking and bore types. Moreover, there is a significant increment in F_{max} that can be caused due to the high flow depth at the impact and the higher flow velocity resulted by the breaking of wave.

Further, it is visible that the acting maximum tsunami force decreases with the type of the building in the order of ‘Building A’, ‘Building B’ and ‘Building C’, which supports the statement that present of openings reduces the maximum tsunami force acting on buildings. Additionally, there is a significant drop in F_{max} in case of ‘Building C’ when compare to the ‘Building B’ which is supposedly due to the increase of opening ratio.

Fig. 8 is prepared in order to quantitatively evaluate the effect of opening ratio on the acting force; which shows F_{max} for the ‘Case B’ and ‘Case C’ against that of ‘Case A’. The approximate relationship for the each combination is indicated in the straight lines with the equation for the relationship by its side. At the same time, the opening ratio r for the front face of the 1st floor of the building is also indicated in the figure. Here, r is calculated as the ratio of total wall area that faces the tsunami and hence, lowers the value of r , higher the openings in the wall will be. It can be understood from the figure that the rate of reduction of tsunami force acting on the structure is almost constant regardless of the wave condition. Therefore, the opening ratio r can be identified as an important physical parameter in estimating the tsunami force acting on a building with openings facing to seaward. At the same time, it can be noticed that the acting tsunami force varies with orientation of the building. In ‘Case C’ the

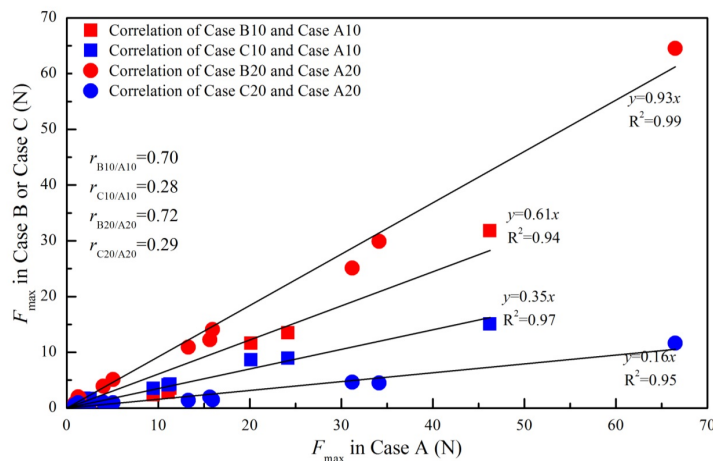


Figure 8. Maximum tsunami force for Case ‘B’ and Case ‘C’ against that of Case ‘A’

orientation which the length side of the building facing tsunami is more effective than width side facing tsunami, in the reduction of total tsunami force, while for 'Case B' it is vice versa. But, in actual scenario, one should not ignore the effect of the inner walls of the building in the estimation of the force. Because the water volume which penetrated into the building can exert some force on the structure while increasing the total force.

Effect of the Internal Arrangement of the Building on Tsunami Force

Two main structural components were considered in the study for the internal arrangement of the building, as a separation wall and an elevator. Each case employed depending upon the position of the structural component is shown in Fig.6. Fig. 9 below depicts the variation of total force acting on the structure plot against that of for the case with no internal arrangement of the building. Fig. 9 (above) pair for the 'Case B' for each orientation separately and Fig. 9 (below) pair shows the same for 'Case C'.

For the 'Case B' it is visible from the figure that, there is no significant increment in the tsunami force with the introduction of elevator or even for its position. This kind of behavior might occur because of the fact that there is still enough space inside the building to make way for the entered water volume. However, in case of internal separation wall, a significant increase in the force can be observed compared to the case with no internal arrangement (Case B11 & Case B12). Understandably, this increment occurred due to the total blockage of penetrated water volume of tsunami due to the presence of the internal separation wall.

For 'Case C' it can be noticed from the figure that the effect of internal arrangement (both elevator shaft and separation wall) is relatively higher than that for 'Case B'. This indicates that the internal structural arrangement which block the tsunami flow, become more influential in estimating the tsunami force, when the openings of the building in the sea side face get larger. Moreover, for the cases with internal separation wall shows much higher increments than the cases with elevator shaft. Further, it is

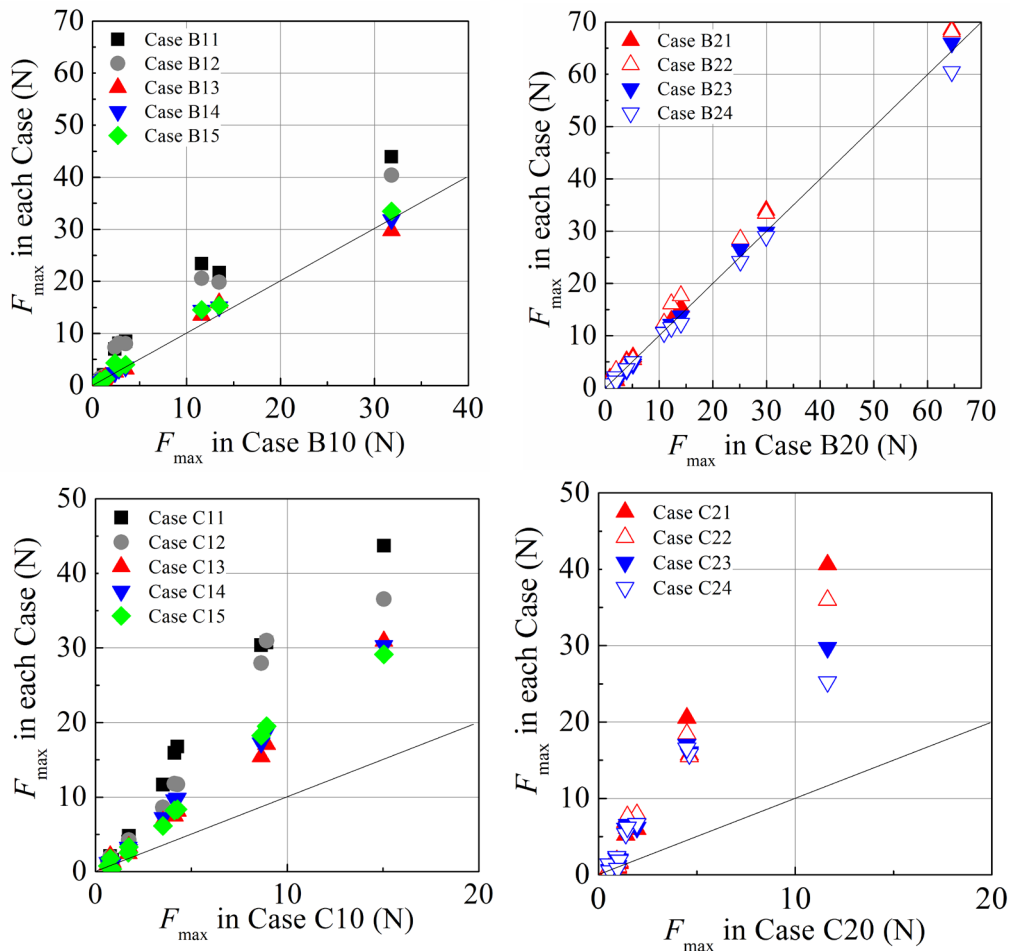


Figure 9. Variation of total tsunami force depending on the internal arrangement of the building

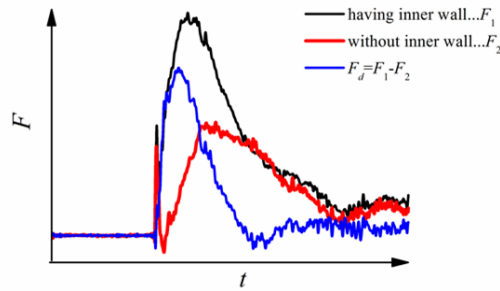


Figure 10. Estimation of the total force on the inner wall

evident that the positioning of the separation wall in the seaward side increases the total tsunami force than that it places in the landward side. Therefore, it is important to have a closer look at the acting pressure distribution on the inner separation wall and elevator shaft to understand this kind of behavior.

The maximum force acting on the inner wall was estimated by deducting the maximum force acting on the building without inner wall from the maximum force acting on the building with the inner wall, as it is graphically explained in Fig. 10. The estimated values for each case are plotted against η_h in Fig. 11, which are categorized depending upon the structure type and its orientation. In the figure it was confirmed from the experiment that generally the higher values for $F_{d\max}$ were observed from the breaking type waves. At the same time it can be noticed that $F_{d\max}$ is increasing with the increase of η_h . Further, higher $F_{d\max}$ is observed for inner separation wall case when compare to the that of for the elevator case, and that can be occurred due to the larger resistance area of the separation wall. It is also evident that $F_{d\max}$ is higher when inner wall positioned in the seaward side when compared with the cases where it is placed in the landward side. Therefore, to minimize the total horizontal force acting on the structure it is recommended that the inner wall to be placed more landward within the structure, rather than place it toward seaward side.

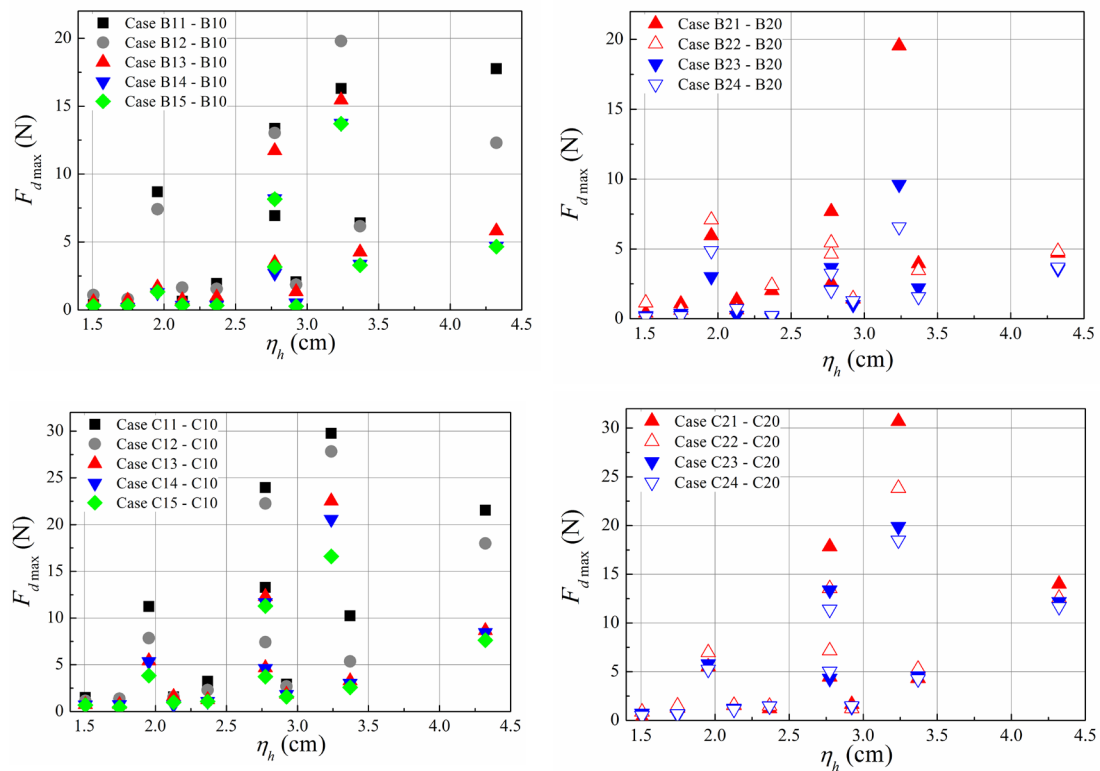


Figure 11. Maximum tsunami force on the inner wall for different cases

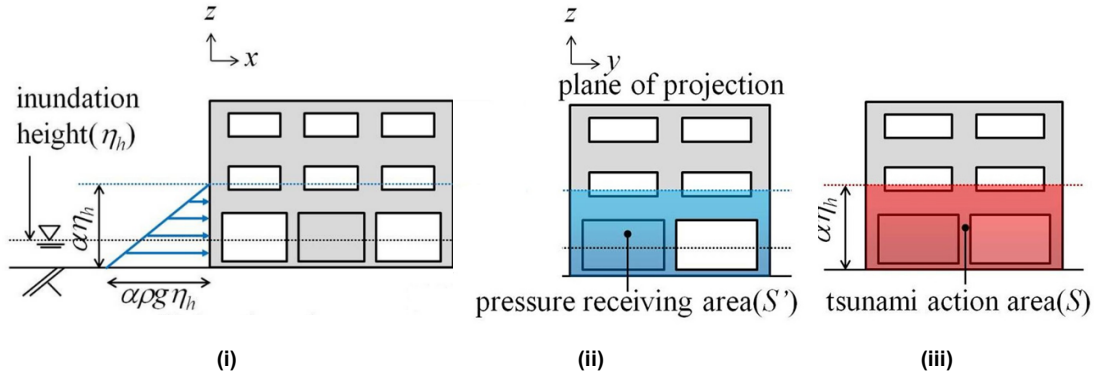


Figure.12 (i) Triangular pressure distribution on the structure; Effective area of tsunami force estimation for (ii) method 1 and (iii) method 2

Tsunami force estimation methods for buildings with openings

In the estimation of the total force acting on the building it was assumed that pressure distribution to be triangular in the vertical direction [Fig. 12 (i)].

The effective height for the pressure action was taken as $\alpha \eta_h$, where η_h is the inundation depth and the α is to be estimated from experiment. For the force calculation two approaches were considered according to the recommendations by the Japanese cabinet office (2012). One approach (method 1) is to estimate the force excluding the pressure action on the areas where openings are present [Fig. 12 (ii)] while the other approach (method 2) is to take the integration of wave pressure without considering the presence of the openings [Fig. 12 (iii)]. The estimated force from the each approach can be expressed as,

Method 1,

$$F_i = \int_{S'} \rho g (\alpha \eta_h - z) ds \quad (2)$$

Method 2,

$$F_r = \frac{S'}{S} \int_S \rho g (\alpha \eta_h - z) ds \quad (3)$$

In the estimation of F_r (Eq. 3), the pressure calculation is multiplied by the ratio of actual pressure receiving area (S') to the tsunami acting area (S). Further, the opening area is calculated as the projected area in the plane perpendicular to the tsunami propagation direction. The estimated tsunami force from the each estimation method is plotted against the F_{max} observed in the experiment for relevant cases are illustrated in Fig. 13. In the calculation the value of α , which is the multiplication factor for the effective water depth, was assumed as 3, as it is the general recommendation. By referring to the figures it can be observed that, the difference between the force estimation from each method is insignificant. Further, estimations for the non-breaking and bore type waves lies within the safe side regardless of the spatial arrangement of the building while the maximum force values for breaking wave condition appear to be under estimated by the proposed methods with $\alpha = 3$.

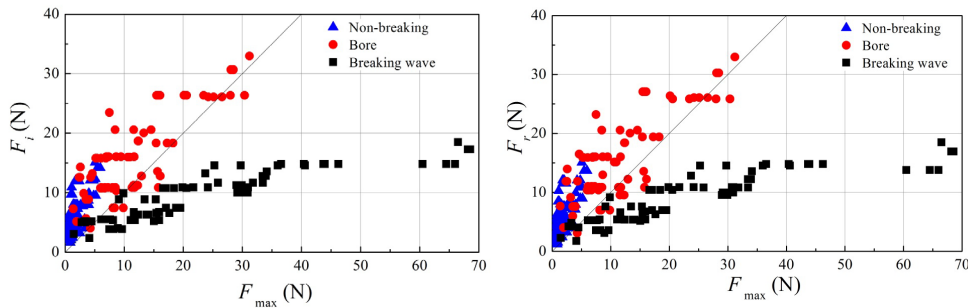


Figure 13. Estimated tsunami force from Method 1 (left) and Method 2 (right) against the measured maximum tsunami force in the experiment

NUMERICAL STUDY

Three-dimensional numerical model developed by Lee et al. (2010) was used for the numerical analysis. In the model, liquid and gas phases are considered to be immiscible and continuity (Eq. 4) and modified Navior-Stokes (Eq. 5) equations are used as governing equations, while free surface is determined by advection equation (Eq. 6) which incorporates VOF method.

$$\nabla \cdot (\theta V) = \tilde{q} \quad (4)$$

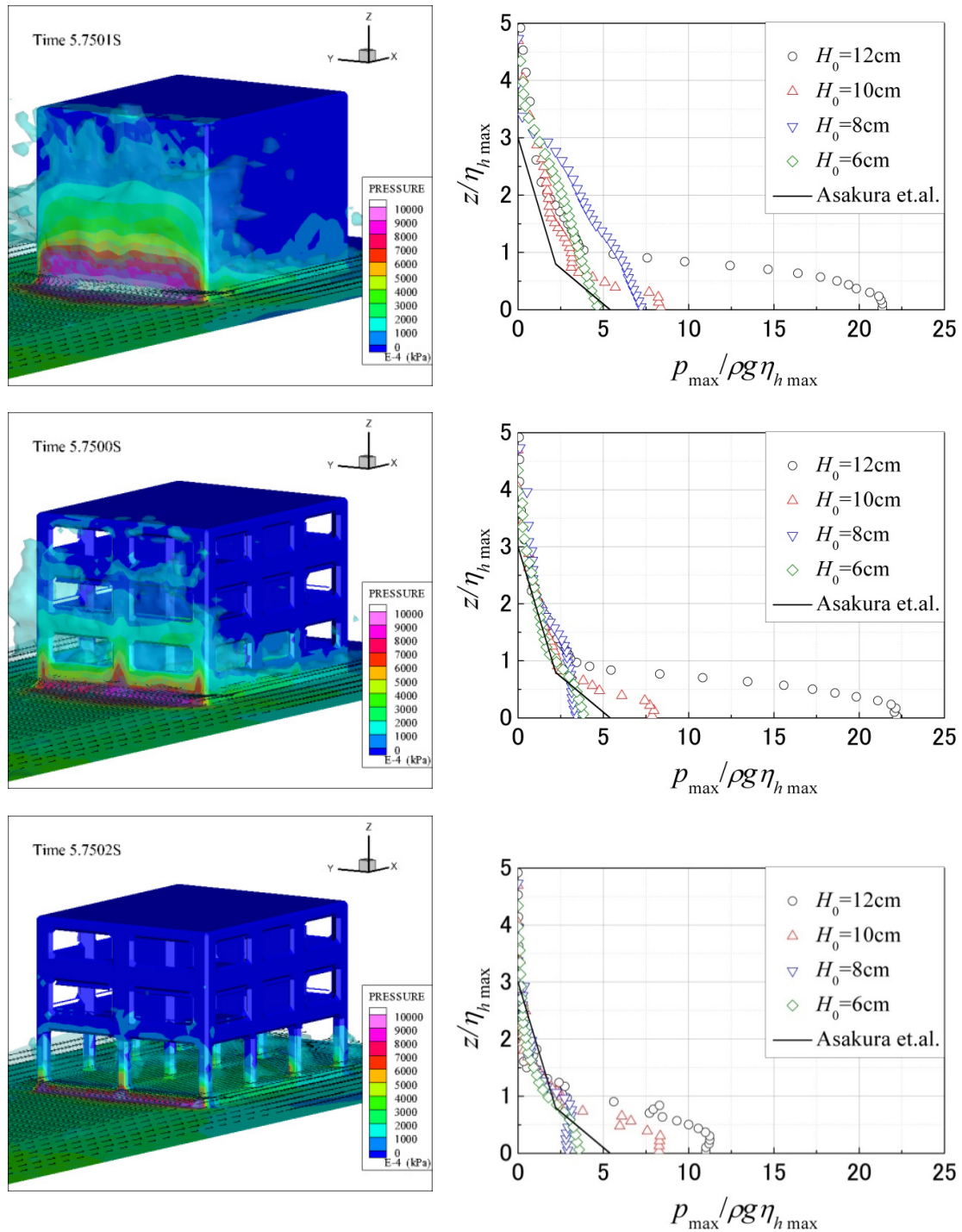


Figure 14. Pressure distribution in graphics (left) and non-dimensional pressure distribution (right) for each case; Case A (top), Case B (Middle) and Case (bottom).

$$\frac{\partial V}{\partial t} + (V \cdot \nabla)V = -\frac{\nabla p}{\rho_w} + \nabla \cdot (2\nu_w E - \tau) - \frac{2}{3} \nabla \{ \nu_w (\nabla V) \} + F_b - \gamma W \quad (5)$$

$$\frac{\partial F}{\partial t} + \nabla V \cdot F = F \tilde{q} \quad (6)$$

where, V : velocity vector, $\tilde{q}=q/\Delta x_s$: source term required to generate wave, q : flux density at wave source position ($x = x_s$), t : time, p : pressure, ρ_w : fluid density, ν_w : kinematic viscosity coefficient, E : strain rate tensor, τ : sub-grid stress vector, F_b : body force such as gravity and surface tension, γ : wave dissipation factor which equals to zero except in the added dissipation zone.

Numerical study was conducted for different initial wave heights (H_0) and Fig. 14 (left) depicts the pressure distribution observed from the numerical simulation for each case. It is clearly evident that the presence of the spaces on the front face of the building reduces the horizontal tsunami force by allowing the water volume to pass through the openings. Meantime, high pressure concentrations can be observed towards the bottom of the structure for Case A and Case B while the reduced effective face area in Case C comparatively reduces pressure load on the structure.

DISCUSSION AND CONCLUSIONS

In this study tsunami force acting on buildings with openings was investigated experimentally and numerically in terms of the effect of external and internal walls.

When consider the wave profile, the maximum wave force acting on the building is higher for the breaking waves compare to the non-breaking conditions. This can be occurred due to the high inundation depth and higher velocity of the breaking wave at the time of impingement with the structure. At the same time, both experimental and numerical results are agreed that the high pressure zone on the building is decreased with the increase of the opening area which indicates that the introduction of pilotis-type buildings is more effective in reducing the tsunami force.

As far as internal arrangements are considered, the maximum tsunami force was increased by the presence of the internal wall, and both maximum tsunami force F_{max} and maximum tsunami force acting on the internal wall $F_{d max}$ tent to increase as its location was moved seaward. Moreover, two tsunami force estimation approaches for a building with openings were assessed and no significant difference between two approaches is discovered. In addition, the importance of a selecting an appropriate vale for the coefficient of the effective depth (α) is highlighted.

ACKNOWLEDGMENTS

This work was supported by JSPS KAKENHI Grant Number 25249067.

REFERENCES

- Asakura T., Iwase K., Ikeya T., Takao M., Kaneto T., Fuji N. and Omori M. (2000): An experimental study on wave force acting on on-shore structures due to overflowing tsunamis, *Proc. of Coastal Eng.*, Vol. 47, pp. 911-915.
- Arikawa T., Ikebe M., Yamada F., Shimosako K. and Imamura F. (2005): Large model test of tsunami force on a revetment and on a land structure, *Ann. J. of Coastal Eng.*, Vol. 52, pp. 746-750.
- Cabinet office of Japanese Government, (2005): The guideline concerning the Tsunami Evacuation.
- Nakano Y. (2008): Design load evaluation for tsunami shelters based on damage observations after Indian Ocean tsunami disaster due to the 2004 Sumatra earthquake, *The 14th World Conference on Earthquake Engineering*, Paper ID 15-0008.
- Lukkunaprasit, P., Ruangrassamee, A. and Thanasisathit, N. (2009): Tsunami loading on building with openings, *Science of Tsunami Hazards*, Vol. 28, No. 5, pp. 303-310
- Lee K. H., Mizutani N. and Kang Y. K. (2010): Applicability of 3D Numerical wave tank to Slit-type caisson breakwater with complex geometry, *Ann. J. of Civil Eng. In the Ocean*, Vol. 26, pp. 69-74.
- Nishiyama I. (2011): Building damage by the 2011 off the pacific coast of Tohoku earthquake and coping activities by NLIM and BRI collaborated with the administration, *US-Japan joint meeting on "Wind and Seismic Effects"*, Tsukuba.